

# Design of a 400 MHz cavity backed CPW fed bow-tie antenna for GPR applications

Nairit Barkataki\*

*Department of Instrumentation & USIC  
Gauhati University  
Guwahati, India  
nairitb@gauhati.ac.in*

Utpal Sarma

*Department of Instrumentation & USIC  
Gauhati University  
Guwahati, India  
utpalsarma@gauhati.ac.in*

Pranjal Borah

*Department of Instrumentation & USIC  
Gauhati University  
Guwahati, India  
pranworld@gmail.com*

Banty Tiru

*Department of Physics  
Gauhati University  
Guwahati, India  
btiru@gauhati.ac.in*

**Abstract**—This study presents the design a 400 MHz CPW-fed bow-tie slot antenna backed by a cavity. The application of UWB signal sources in ground penetrating radar (GPR) is widely recognised. The antennas are first modelled and simulated, and then tested using a VNA. The antenna has a high gain and very good (F/B) ratio. The antenna exhibits resonance at 401 MHz and 421 MHz and has a measured bandwidth of 47.5%. It has a realised gain of 6.68 dB at 400 MHz.

**Index Terms**—bow-tie, antenna, ground penetrating radar

## I. INTRODUCTION

GPR is a non-destructive technique (NDT) that is commonly used to detect buried objects. It has a wide range of applications, including soil property estimation, snow, ice and glacier property estimation, archaeological site non-destructive inspection imaging, well inspection, investigation of road conditions, tunnel lining and mine detection [1].

The total energy efficiency of the GPR system is heavily influenced by the performance of the antenna used to transmit and receive radio frequency (RF) signals. It's also worth noting that all basic parameters show frequency-related behaviour. In contrast to telecommunications antennas, which are designed for use in free space, GPR antennas work very close to the ground. As a result, the performance of these antennas varies depending on the type of soil.

A GPR system's antenna must have high gain, be small in size and have ultra-wideband (UWB) capabilities. There are only a few types of antennas that can fulfil such specifications like bow-tie, TEM horn, cone-slot, spiral, and Vivaldi antennas. There is always an ideal compromise between the required depth of penetration and resolution as obtaining a low frequency of operation (penetration depth) and UWB performance (resolution) are mutually exclusive goals. It is usually advisable to create and design the antenna for the specific application, taking into consideration the desired range and , resolution.

This work was supported by DST (Govt. of India) under DST FIST Scheme  
\*Corresponding author

Guo et al. developed a UWB Vivaldi antenna for a GPR system. It had tapered slots with a working spectrum ranging from 300 MHz to 2 GHz, with gains ranging from 4.4 to 11.5 dBi [2]. Despite its excellent performance, the 45 cm × 60 cm size was quite big to be constructed with FR4 boards, which come in 30 cm × 30 cm sizes.

The antenna designed by Raza et al. had a wide bandwidth of 0.6-4 GHz and a peak gain of 4 dB [3]. For wideband characteristics, tapered slot feeding, curved ground plane, and slot loading were used, while resistive loading is used to remove the notch band. It measure 180 × 220 mm in total.

Bow-tie antennas have been widely investigated in various literature due to their simple construction, broad impedance bandwidth, and ease of manufacturing. A broad range of designs bow-tie antennas have been presented over the years [4], [5]. They are used in the flagship products of major GPR manufacturers as well. Ke Li et al. proposed a bow-tie antenna design with a frequency range of 200 MHz to 600 MHz [6]. Its physical dimensions were 343 mm x 192 mm. Its gain ranged from -12 dB at 200 MHz to about 2 dB at 600 MHz. End reflection was suppressed using resistive loading. Parallel transmission cables linked to a SMA connection were used to feed the antenna.

Momin et al. designed a wideband bow-tie antenna with a maximum gain of 5 dB at 400 MHz that could operate from 200 MHz to 800 MHz [7]. The antenna structure was a modified bow-tie structure printed on a dielectric substrate. The arm edges of a traditional bow-tie antenna were rounded and notched as part of the alteration.

Liu et al. presented a cavity-backed bow-tie antenna [8]. To increase its performance, a dielectric loading was applied. The antenna had a spectrum of 1-4 GHz with a gain of 5–9 dBi. A design for a high gain bow-tie antenna was proposed by Li et al. which operated in the 348-772 MHz frequency band [9]. They used metamaterial lens and AMC reflector to improve the gain characteristics of the antenna. The side length of the antenna substrate (square) was 420 mm. The antenna had a

gain of 6.5 dB and a F/B ratio of 23 dB.

Co-planar waveguide (CPW) feeding is favoured for balanced output antennas, and for a variety of other reasons such as simplicity of manufacturing, impedance matching, and so on [1]. Ungrounded CPW is commonly employed in GPR antennas since the antenna side contacting the earth's surface lacks a ground plane. They cannot be printed on the same PCB as the accompanying electronics even if they have a planar structure due to impedance mismatch and feeding problems. The addition of artificial materials to the antenna design process, such as loading elements, further complicates the design.

#### Aim of present work

This study presents the design a CPW-fed bow-tie slot antenna backed by a cavity. The goal is to get an optimised size of the antenna which may have reduced dimensions than those of the reported ones. Proper matching of the CPW length, width and the slot gap may help in reducing the overall size of the antenna. Modelled and designed to operate at a centre frequency of 400 MHz, the antenna is fabricated on FR4.

## II. METHODOLOGY

### A. Antenna Design

The bow-tie antenna's properties are mostly determined by angles. The geometry, as shown in Fig. 1 of a bow-tie antenna is characterised by three factors [5]

- flare angle  $\theta_0$
- gap distance  $g$
- arm length  $a$

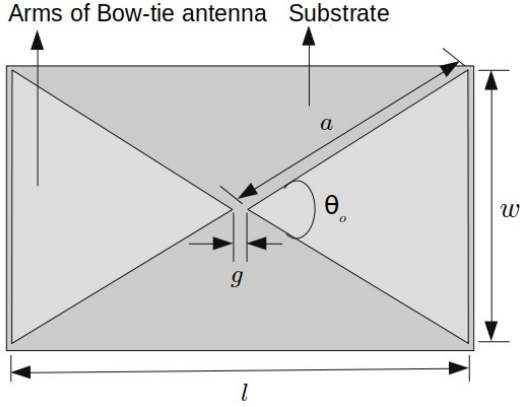


Fig. 1. Geometry of the bow-tie antenna

The bow-tie antenna's characteristic impedance is largely determined by the flaring angle and is given by [4] as

$$Z_c = 120 \ln \left( \cot \left( \frac{\theta_0}{4} \right) a \right) \quad (1)$$

where  $\theta_0$  is the flare angle. Antenna length  $l$  can be determined by:

$$l = \lambda_0 \times \left( \frac{1}{\sqrt{\epsilon_{eff}}} \right) \quad (2)$$

where  $\lambda_0$  is the wavelength of the lowest frequency. The following expression can be used to estimate the effective relative permittivity. [4]:

$$\epsilon_{eff} = \left( \frac{\epsilon_r + 1}{2} \right) + (\epsilon_r - 1) \left( 1 + \left( 10 \frac{h}{w} \right) \right)^{-0.5555} \quad (3)$$

where  $w$  (mm) is the antenna width in mm,  $h$  is the substrate thickness in mm,  $\epsilon_r$  is the dielectric constant of the substrate.

CPW characteristic impedance,  $Z_0$ , is calculated as specified in [1]:

$$Z_0 = \left( \frac{30 \times \pi}{\sqrt{\epsilon_{eff}}} \right) \left( \frac{K(k')}{K(k)} \right) \quad (4)$$

where

$$\epsilon_{eff} = 1 + \left\{ \frac{(\epsilon_r - 1)}{2} \right\} \left\{ \left( \frac{K(k')}{K(k)} \right) \left( \frac{K(k_1)}{K(k_1')} \right) \right\} \quad (5)$$

$$k = \frac{w_{cpw}}{w_{cpw} + 2S_{cpw}} \quad (6)$$

$$k_1 = \frac{\sin h \left( \frac{\pi w_{cpw}}{4h} \right)}{\sin h \left( \frac{(w_{cpw} + 2S_{cpw})\pi}{4h} \right)} \quad (7)$$

$$k' = \sqrt{1 + k^2} \quad (8)$$

Here,  $k$  denotes complete elliptic integral of the first kind,  $w_{cpw}$  is the central strip width,  $S_{cpw}$  is the gap width of the CPW line and  $h$  is the height of the substrate, as shown in Fig. 2.

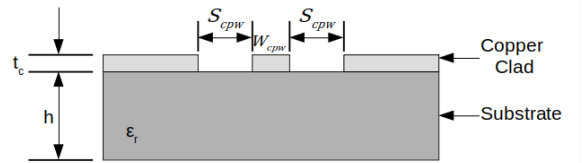


Fig. 2. Dimensions of the coplanar waveguide

By using the eqs. (1) to (8), the design parameters of the CPW line and antenna are calculated.

Fig. 3 shows the geometry of the proposed antenna. This antenna is constructed using a copper-coated FR4 substrate. The copper cladding is  $t_c = 0.035$ mm thick. The antenna is backed by a cavity made of aluminium. 2 strips of Plexiglas ( $\epsilon_r=3.6$ ) of dimensions  $30 \text{ mm} \times L'$  are used to support the antenna so that it is easier to attach it to the cavity

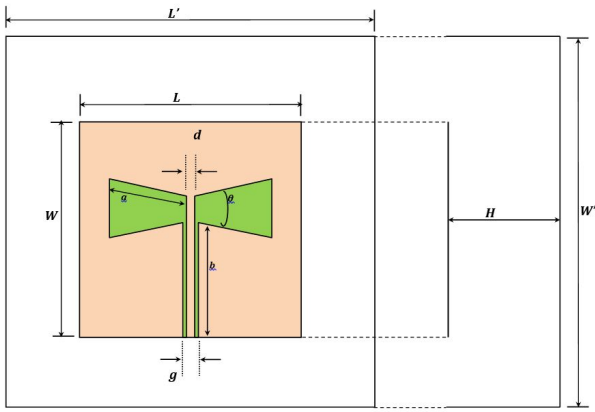


Fig. 3. Design of the bow-tie antenna

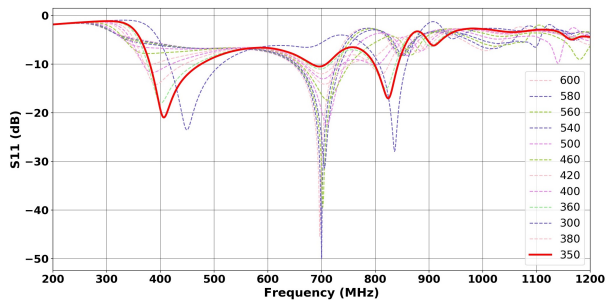


Fig. 4. Return loss plotted for different values of cavity length

### B. Parameter Sweep

The initial length ( $L' = 580$  mm) and width ( $W' = 400$  mm) of the cavity are taken as twice the dimensions of the antenna substrate. The following parameters are then varied through a range of values to get the best result loss at 400 MHz and a reasonably wideband for good performance.

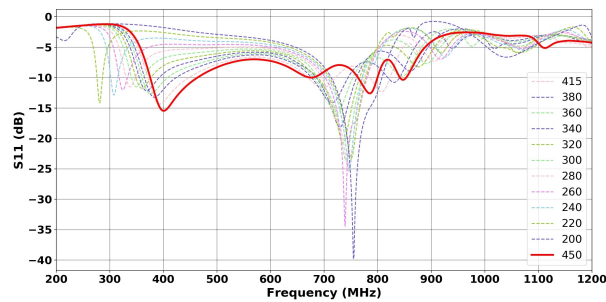


Fig. 5. Return loss plotted for different values of cavity width

- Cavity length - 300 to 600 mm
- Cavity width - 200 to 450 mm
- Cavity height - 140 to 220 mm
- Flare angle -  $15^\circ$  to  $30^\circ$
- Inner width of the CPW feed line - 1.5 to 3.0 mm
- Outer width of the CPW feed line - 4.0 to 8.0 mm

To begin with, the cavity length ( $L'$ ) is changed from 300 to 600 mm in increments of 5 mm. The other parameters are

kept at the initial values as obtained from eqs. (1) to (8). Plots for variation of return loss are shown in Fig. 4 for some of the values of cavity length. The best return loss is obtained for  $L' = 350$  mm.

The cavity length is now changed to 350 mm and cavity width ( $W'$ ) is varied from 200 to 450 mm in increments of 5 mm. Plots for variation of return loss are shown in Fig. 5 for some of the values of cavity width. The best return loss is obtained for  $W' = 450$  mm.

Keeping  $L' = 350$  mm and changing  $W'$  to 450 mm, the flare angle ( $\theta_f$ ) is now varied from  $15^\circ$  to  $30^\circ$ . Plots for variation of return loss for some of the values of cavity width are shown in Fig. 6. The best return loss is obtained for  $\theta_f = 27^\circ$ .

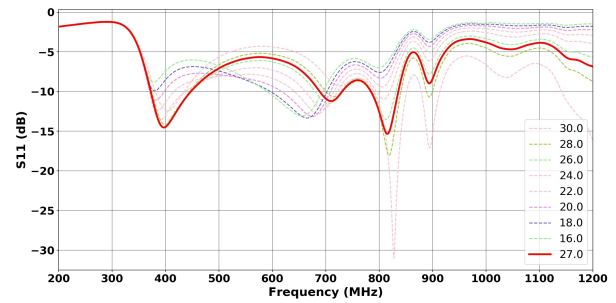


Fig. 6. Return loss plotted for different values of flare angle

For  $L' = 350$  mm,  $W' = 450$  mm and  $\theta_f = 27^\circ$ , the inner width of the CPW feed line ( $d$ ) is now changed from 1.5 to 3.0 mm in increments of 1 mm. Plots for variation of return loss for some of the values of  $d$  are shown in Fig. 7. The best return loss is obtained for  $d = 1.5$  mm.

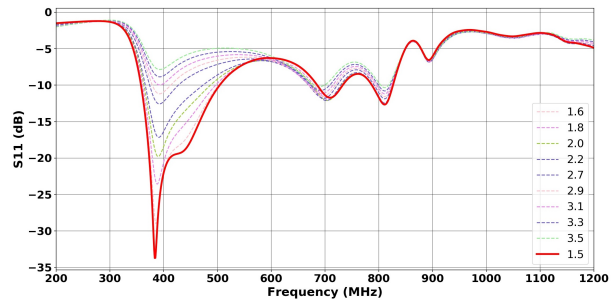


Fig. 7. Return loss plotted for different values of  $d$

For  $L' = 350$  mm,  $W' = 450$  mm,  $\theta_f = 27^\circ$  and  $d = 1.5$  mm, the outer width of the CPW feed line ( $g$ ) is varied from 4 to 8 mm in increments of 1 mm. Plots for variation of return loss for some of the values of  $g$  are shown in Fig. 8. The best return loss is obtained for  $g = 6.7$  mm.

For  $L' = 350$  mm,  $W' = 450$  mm,  $\theta_f = 27^\circ$ ,  $d = 1.5$  mm and  $g = 6.7$  mm, the cavity height ( $H$ ) is varied from 140 to 220 mm in increments of 5 mm. Plots for variation of return loss are shown in Fig. 9 for some of the values of cavity height. The best return loss is obtained for  $H = 145$  mm.

Finally, the design parameters obtained from the parameter sweep are optimised using particle swarm optimization (PSO)

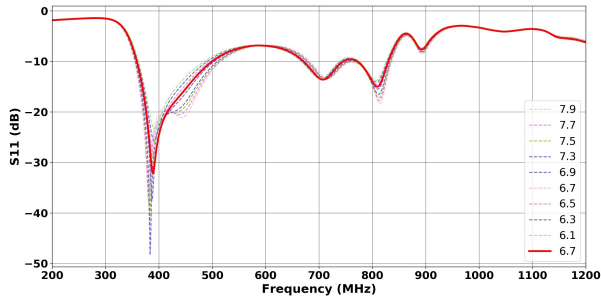


Fig. 8. Return loss plotted for different values of  $g$

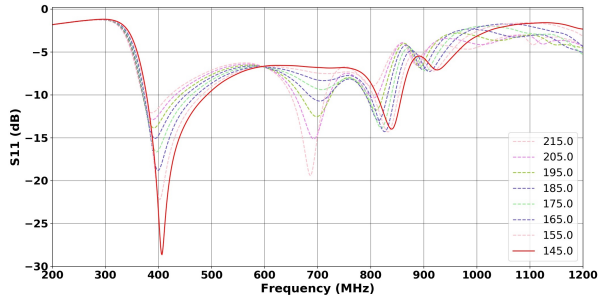


Fig. 9. Return loss plotted for different values of  $H$

algorithm. PSO is an algorithm for optimizing a problem by iteratively attempting to enhance a solution in terms of a given quality measure. It has proved to be effective in optimising a wide range of antennas designs, and it is a robust and stochastic search method [10], [11].

In this work, PSO is used to optimised the design parameters for lowest return losses at resonance frequency of 400 MHz, a wide bandwidth, and a high gain. Fig. 10 shows the return loss of the antennas before and after optimisation.

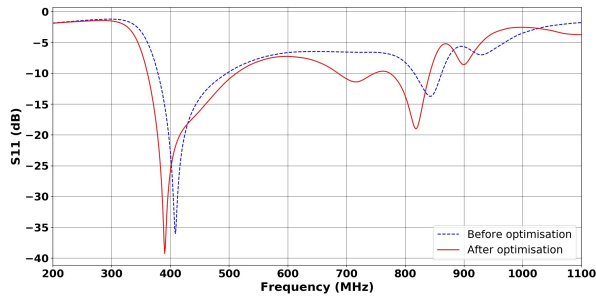


Fig. 10. Return loss using optimised design parameters

The final optimised dimensions are shown in Table I.

Fig. 11 shows the bow-tie antenna with cavity, fabricated on a single sided FR4 copper clad board of thickness 1.6 mm.

### III. RESULTS

#### A. Return Loss ( $S_{11}$ )

The fabricated antenna's return loss is measured using a Keysight FieldFox N9923A VNA. Fig. 12 shows the simulated and experimental return loss plots of the antenna.

TABLE I  
OPTIMISED DESIGN PARAMETERS FOR THE PROPOSED ANTENNA

Parameters	Symbols	Values
Arm Length	$a$	134.56 mm
Flare angle	$\theta_f$	$25^\circ$
Length of CPW feed line	$L_g$	133.00 mm
Inner width of the CPW feed line	$d$	3.00 mm
Outer width of the CPW feed line	$g$	7.50 mm
Length of the substrate	$L$	290.00 mm
Width of the substrate	$W$	200.00 mm
Height of the substrate	$h$	1.6 mm
Height of the conductor, Cu layer	$t_c$	0.035mm
Dielectric constant of the substrate	$\epsilon_r$	4.3
Length of the cavity	$L'$	380.00 mm
Width of the cavity	$W'$	410.00 mm
Height of the cavity	$H$	175.00 mm



Fig. 11. Fabricated bow-tie antenna

Based on our simulations, the -10dB bandwidth covers a range from 361 MHz to 512 MHz (37.35%) with a minimum return loss of -39.24 dB at 390 MHz. The measured bandwidth ranges from 365 MHz to 551 MHz ( $\sim 46.5\%$ ) with minimum return loss of -34.47 dB at 421 MHz. The difference between the simulated and measured findings might be ascribed to fabrication tolerance.

#### B. Gain

Figures 13 and 14 depict the antenna's radiation patterns simulated in E-plane ( $\Phi = 0^\circ$ ) and H-plane ( $\Phi = 90^\circ$ ). In the endfire direction, the antenna has a high gain. Its high gain coupled with a front-to-back (F/B) ratio of 27.78 dB will certainly make it an ideal antenna for GPR since the signal will be able to penetrate deeper into the ground.

### IV. CONCLUSION

The simulated and experimental results of a 400 MHz cpw fed bow-tie antenna are presented in this study. A VNA is used to test the antennas after they have been designed and modelled using HFSS. It is seen that matching performance

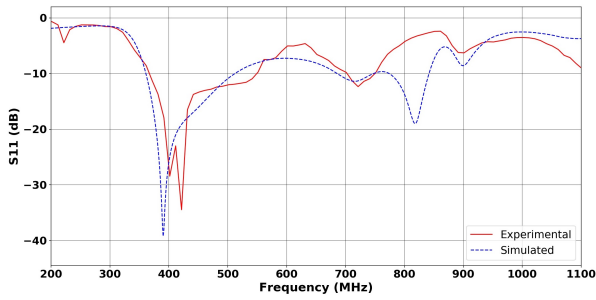


Fig. 12. S-Parameters of the bow-tie antenna

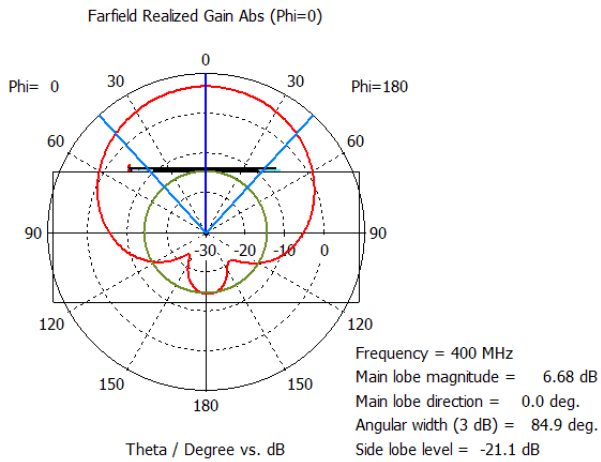


Fig. 13. Simulated radiation pattern for  $\Phi=0^\circ$

degrades on directly reducing the dimensions of the substrate. Proper matching of the feedline length, width, and slot gap aid in optimising the size of the antenna and the reflector. The optimised antenna has smaller dimensions, higher gain, and a better F/B ratio than previously reported designs. The antenna exhibits resonance at 401 MHz (-28.43 dB) and 421 MHz (-34.47 dB). The observed results (46.5%) outperform the simulated outcomes (37.75%) in terms of bandwidth. At 400 MHz, it has a realised gain of 6.68 dB. Its wide bandwidth, high gain, and high F/B ratio makes it an ideal choice for for imaging with high-resolution and deep penetration. In comparison to other antenna types, the bow-tie antenna's planar construction, compact form factor, and lightweight design makes it easier to incorporate within the enclosure housing other GPR equipment.

Based on the data in table II, in comparison to other UWB antennas, the proposed antenna is simple to build, low cost, and has high gain and directivity.

GPR pulses, produced by applying a step function voltage, have large instantaneous bandwidth. This causes ringing effect in conventional antennas. When this impact is significant, deeper objects of interest may be entirely hidden in a GPR survey. This phenomenon can be mitigated by introducing resistive loading to the antenna. The authors intend to enhance the current design by decreasing the ringing impact.

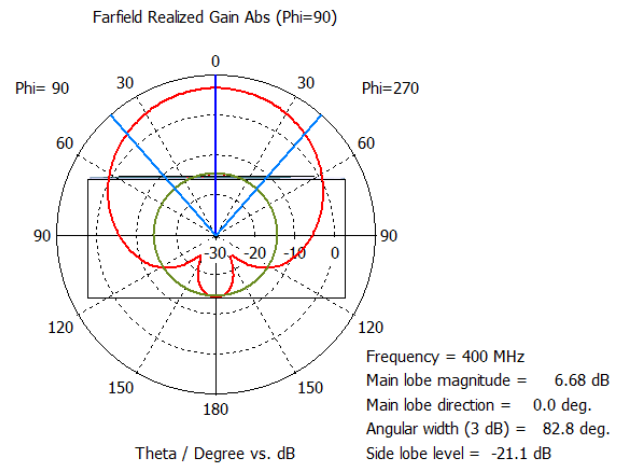


Fig. 14. Simulated radiation pattern for  $\Phi=90^\circ$

TABLE II  
ANTENNA PERFORMANCE PARAMETERS COMPARED WITH REPORTED LITERATURE

Author	Structure	Frequency (GHz)	Max Gain (dB)	Ease of fabrication
Richardson et al. [12]	cavity backed spiral (3D)	0.75-1.25	6	complex
Guo et al. [13]	Vivaldi with exponential tapered slots (planar)	0.3-2	11.5	simple but large size
Liu et. al. [8]	cavity backed bow-tie with dielectric loading (3D)	1-4	9	complex
Li et. al. [9]	slotted bow-tie with AMC & metamaterial lens (planar)	0.35 - 0.77	6.5	complex
Proposed antenna	cavity backed CPW fed bow-tie (planar)	0.36 - 0.55	6.68	Simple and low cost

#### ACKNOWLEDGEMENT

The authors thank Anil Kumar Rajak, Hafizuddin Ahmed, Hridoy Jyoti Saikia and Tilak Chandra Deka for their help during fabrication of the antenna. The authors also thank Sujit Chatterjee and Sharmistha Mazumdar for helping in testing of the antenna and in visualising the results.

#### REFERENCES

- [1] R. Nayak and S. Maiti, "A review of bow-tie antennas for gpr applications," *IETE Technical Review*, pp. 1–16, 2018.
- [2] J. Guo, J. Tong, Q. Zhao, J. Jiao, J. Huo, and C. Ma, "An ultrawide band antipodal vivaldi antenna for airborne gpr application," *IEEE Geoscience and Remote Sensing Letters*, vol. 16, no. 10, pp. 1560–1564, 2019.
- [3] A. Raza, W. Lin, Y. Chen, Z. Yanting, H. T. Chattha, and A. B. Sharif, "Wideband tapered slot antenna for applications in ground penetrating radar," *Microwave and Optical Technology Letters*, vol. 62, no. 7, pp. 2562–2568, 2020.
- [4] R. Nayak, S. Maiti, and S. K. Patra, "Design and simulation of compact uwb bow-tie antenna with reduced end-fire reflections for gpr applications," in *2016 International Conference on Wireless Communications, Signal Processing and Networking (WiSPNET)*. IEEE, 2016, pp. 1786–1790.

- [5] N. Barkataki, B. Tiru, and U. Sarma, "Performance investigation of patch and bow-tie antennas for ground penetrating radar applications," *International Journal of Advanced Technology and Engineering Exploration*, vol. 8, no. 79, p. 753, 2021.
- [6] K. Li, T. Dong, and Z. Xia, "Improvement of bow-tie antenna for ground penetrating radar," in *2019 International Conference on Microwave and Millimeter Wave Technology (ICMMT)*. IEEE, 2019, pp. 1–3.
- [7] S. M. Momin, A. P. Khandare, S. Sawarkar, and D. Pethe, "Design of high performance & wide-bandwidth bow-tie antenna for ground penetrating radar (gpr) system," in *2019 IEEE Pune Section International Conference (PuneCon)*. IEEE, 2019, pp. 1–5.
- [8] S. Liu, M. Li, H. Li, L. Yang, and X. Shi, "Cavity-backed bow-tie antenna with dielectric loading for ground-penetrating radar application," *IET Microwaves, Antennas & Propagation*, vol. 14, no. 2, pp. 153–157, 2020.
- [9] Y. Li and J. Chen, "Design of miniaturized high gain bow-tie antenna," *IEEE Transactions on Antennas and Propagation*, 2021.
- [10] A. Hamid and W. Obaid, "Hexa-band mimo cpw bow-tie aperture antenna using particle swarm optimization," *International Journal of Electrical and Computer Engineering (IJECE)*, vol. 8, no. 5, pp. 3118–3128, 2018.
- [11] X. Jia and G. Lu, "A hybrid taguchi binary particle swarm optimization for antenna designs," *IEEE Antennas and Wireless Propagation Letters*, vol. 18, no. 8, pp. 1581–1585, 2019.
- [12] M. Richardson, C. J. Bauder, R. Kazemi, and A. E. Fathy, "Design of a rigid uwb log spiral antenna for gpr applications in harsh environment," in *2020 IEEE Radio and Wireless Symposium (RWS)*. IEEE, 2020, pp. 262–264.
- [13] P. Guo, H. Ma, R. Chen, and D. Wang, "A high-efficiency fpga-based accelerator for binarized neural network," *Journal of Circuits, Systems and Computers*, vol. 28, no. supp01, p. 1940004, 2019.